Bioorganic & Medicinal Chemistry Letters 22 (2012) 679–682

Contents lists available at SciVerse ScienceDirect

Bioorganic & Medicinal Chemistry Letters

journal homepage: www.elsevier.com/locate/bmcl

Characterisation of [^{11}C]PR04.MZ in *Papio anubis* baboon: A selective high-affinity radioligand for quantitative imaging of the dopamine transporter

Patrick J. Riss [a,b,*], Jacob M. Hooker [c], Colleen Shea [c], Youwen Xu [c], Pauline Carter [c], Donald Warner [c], Valentina Ferrari [b], Sung-Won Kim [c], Franklin I. Aigbirhio [b], Joanna S. Fowler [c], Frank Roesch [a]

[a] *Institute of Nuclear Chemistry, Johannes Gutenberg University, Fritz-Strassmann-Weg 2, D-55128 Mainz, Germany*
[b] *Wolfson Brain Imaging Centre, Department of Clinical Neurosciences, University of Cambridge, Cambridge, CB2 0QQ, United Kingdom*
[c] *Medical Department, Brookhaven National Laboratory, Upton, NY 11973, USA*

ARTICLE INFO

Article history:
Received 26 August 2011
Revised 13 October 2011
Accepted 14 October 2011
Available online 25 October 2011

Keywords:
Dopamine transporter
PET imaging
Carbon-11
Non-human primates

ABSTRACT

N-(4-fluorobut-2-yn-1-yl)-2β-carbomethoxy-3β-(4′-tolyl)nortropane (PR04.MZ, **1**) is a PET radioligand for the non-invasive exploration of the function of the cerebral dopamine transporter (DAT). A reliable automated process for routine production of the carbon-11 labelled analogue [^{11}C]PR04.MZ ([^{11}C]-**1**) has been developed using GMP compliant equipment. An adult female *Papio anubis* baboon was studied using a test–retest protocol with [^{11}C]-**1** in order to assess test–retest reliability, metabolism and CNS distribution profile of the tracer in non-human primates. Blood sampling was performed throughout the studies for determination of the free fraction in plasma (f_P), plasma input functions and metabolic degradation of the radiotracer [^{11}C]-**1**. Time–activity curves were derived for the putamen, the caudate nucleus, the ventral striatum, the midbrain and the cerebellum. Distribution volumes (V_T) and non-displaceable binding potentials (BP_{ND}) for various brain regions and the blood were obtained from kinetic modelling. [^{11}C]-**1** shows promising results as a selective marker of the presynaptic dopamine transporter. With the reliable visualisation of the extra-striatal dopaminergic neurons and no indication on labelled metabolites, the tracer provides excellent potential for translation into man.

Presynaptic membrane transporter mediated neurotransmitter reuptake is crucial for the mediation of monoamine signal transduction.[1] Imaging of the neurotransmitter sodium symporters with positron emission tomography (PET) provides valuable insights into reuptake dysfunction and function of the neuron.[2–5] PET studies of the dopamine transporter (DAT) provide information on the presynaptic integrity of the dopaminergic system in psychiatric and movement disorders. Radiolabelled DAT-ligands are established for the early clinical diagnosis of Parkinson's disease (PD) and the differentiation of PD from symptomatically related disorders. A variety of compounds has already been evaluated and utilised for studies of the striatal DAT. Cocaine derived phenyltropanes have emerged from these studies as the most appropriate imaging agents for this purpose. However, particular limitations of these agents include low selectivity of the ligand over the serotonin transporter (SERT) and the norepinephrine transporter (NET), blood brain barrier penetrating metabolites, non-specific binding and slow binding equilibrium.[6,7] Moreover, there is an unmet need for a high affinity radioligand suitable for the visualisation of low density DAT populations outside the striatum particularly given the fact that the dopaminergic signal pathways originate in the midbrain and dopaminergic degradation in the substantia nigra causes the downstream effects of PD in the striatum. This brain region also shows pathologic alterations in children with attention deficit/hyperactivity syndrome (ADHS).[9b] Nevertheless, only a few DAT studies targeting the midbrain region, have been performed due to the absence of appropriate imaging agents.

We were interested in the cerebral distribution, metabolism and initial kinetic modelling results of N-(4-fluorobut-2-yn-1-yl)-2β-carbomethoxy-3β-(4′-tolyl)nortropane (PR04.MZ, **1**), a promising radiotracer from our laboratories,[10] in non-human primates.

PR04.MZ is a high affinity ($IC50_{hDAT}$: 2 nM) DAT-selective (SERT/DAT-selectivity: >50; NET/DAT-selectivity: >10) competitive inhibitor of monoamine reuptake but not a substrate for the DAT.

Its affinity exceeds the figures reported for other established DAT-ligands, such as PE2I (K_d(rat): 4 nM),[12] FECNT (K_i: 8 nM)[8] or LBT-999 (K_d(rat): 9 nM).[12] Moreover, indications of superior selectivity have been reported recently.[15] In vitro monoamine transporter inhibition potency and selectivity as well as an experimental log*D* value of **1** are summarised in Table 1.[13] The molecular structure of **1** provides two sites for the straightforward incorporation of either carbon-11 or fluorine-18. Radiolabelling with both PET nuclides has been communicated recently.[10] Moreover, an automated process for the production of the carbon-11 labelled radiotracer [^{11}C]-**1** has been developed to facilitate upcoming human studies.

* Corresponding author.
E-mail address: pr340@wbic.cam.ac.uk (P.J. Riss).

0960-894X/$ - see front matter © 2011 Elsevier Ltd. All rights reserved.
doi:10.1016/j.bmcl.2011.10.053

Table 1
In vitro data for PR04.MZ; IC_{50} values were obtained from hDAT, hSERT and hNET stably transfected in HEK 293 cell lines, [^{3}H]Dopamine ([^{3}H]DA) and [^{3}H]WIN 35,428 were used at the DAT, [^{3}H]Serotonin ([^{3}H]5-HT) and [^{3}H]Citalopram were used at the SERT, [^{3}H]Noradrenalin ([^{3}H]NE) and [^{3}H]Nisoxetine were used at the NET[a]

$hDAT_{IC50}$ [^{3}H]DA ([^{3}H]WIN) nM	$hSERT_{IC50}$ [^{3}H]5-HT([^{3}H]Citalopram) nM	$hNET_{IC50}$ [^{3}H]NE ([^{3}H]Nisoxetine) nM	% unbound in plasma	log $D_{7.4}$ HPLC[13]
3.26 ± 0.49 (1.93 ± 0.2)	239.77 ± 3.67 (108.4 ± 1.3)	31.04 ± 0.58 (22.48 ± 0.83)	4.4 ± 0.1	2.7 ± 0.2

[a] see 10a for experimental details and reference data for established DAT ligands

Automated radiosynthesis of [^{11}C]PR04.MZ. [^{11}C]CO_2 was produced via proton bombardment of an enriched [^{14}N]N_2 target using the ^{14}N(p,a)^{11}C nuclear reaction. [^{11}C]PR04.MZ was produced under GMP compliant conditions using a GE tracerlab® FX_C synthesis module, adapted to the captive solvent method (Schemes 1 and 2).[11]

Labelling precursor **2** (0.1 mg) and TBAOH (2 equiv) in 100 µl DMF were loaded into the HPLC-loop of the synthesis module. [^{11}C]CH_3I was passed through the loop in a stream of nitrogen (25 ml min^{-1}) for 2 min followed by a reaction time of 1 min after which the remaining contents of the loop were injected into the built-in preparative HPLC. Radiotracer was purified within 14 min, isolated via solid phase extraction using an SCX cartridge and formulated in sterile phosphate buffered saline (PBS). Overall synthesis duration from end of bombardment (EOB) was 30 min.

[^{11}C]PR04.MZ was obtained in a yield of 9.1 ± 4.8%. The product formulation was a colourless, clear solution with a specific activity of 185 ± 30 MBq/nmol. The radiochemical purity exceeded 97%. The chemical purity was >95%.[24]

Primate imaging. To evaluate and validate [^{11}C]-**1** in primates, extra-striatal binding, test–retest reliability and plasma metabolism were investigated in a female *Papio anubis* baboon.

Dynamic PET scans were conducted following a test–retest protocol. To maintain minimum variability of the experimental conditions, a test–retest scan was conducted with [^{11}C]-**1** in the same baboon on the same day using a Siemens ECAT HR+PET scanner. The animal was anaesthetised using isoflurane and vital body functions were monitored throughout the scan. Under test–retest conditions, the acquisition time was 90 min for both scans. The subject was allowed to rest for 30 min between the scans. In total, three scans were conducted with 137.4 ± 66.8 MBq of [^{11}C]-**1**. The initial frames of the PET study were summed and used for a PET–PET fusion with an H_2[^{15}O]O brain perfusion scan, co-registered with an MRI atlas of the baboon brain. Regions of interest were drawn onto the anatomic MRI image and copied to the dynamic PET data. Time activity curves for putamen, caudate nucleus, ventral striatum, midbrain and cerebellum are shown in Figure 1.

Automated blood sampling was performed throughout the studies for plasma input and metabolite analysis.[17] Metabolite-corrected plasma input functions were derived from the blood samples. Distribution volumes (V_T) for various brain regions were obtained from Logan-plot analysis and non-displaceable binding potentials (BP_{ND}) were computed.[20–22]

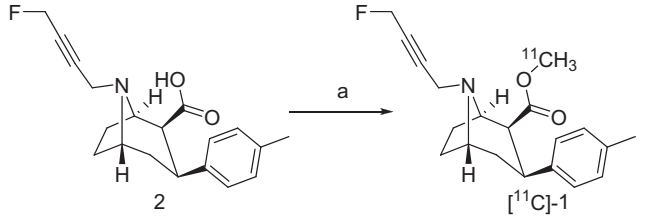

Scheme 1. Radiosynthesis of [^{11}C]PR04.MZ using [^{11}C]CH_3I. (a) DMSO, TBAOH, [^{11}C]CH_3I, rt, 3 min.

The radiotracer [^{11}C]-**1** shows a rapid accumulation into the DAT-rich brain regions followed by differential washout rates among the different regions of interest (Fig. 1). Labelled **1** shows a high uptake into the DAT-rich brain regions (cf. Fig. 1, a and b), such as the putamen (7.6 ± 0.2%ID/100 ml, 25 ± 2.5 min p.i.) and the caudate nucleus 6.7 ± 0.2%ID/100 ml, 25 min p.i.). The whole brain uptake peaked in the early time frames (26.1 ± 3.5%ID/100 ml, 3 ± 0.5 min p.i.).

The high striatal uptake of 7.6 ± 0.2%ID/100 ml, 25±2.5 min p.i., is reduced to 6.7 ± 0.4% after 90 min and to 4.8% after 180 min. Uptake into the ventral striatum peaked with 3.8 ± 0.4%ID/ml at 7.5 ± 0.5 min followed by continuous washout to 3.1 ± 0.3%ID/ml after 45 min and 2.55 ± 0.2%ID/ml after 90 min. The midbrain region shows a peak uptake of 2.8 ± 0.2%ID/ml after 3.5 min which is reduced to 1.3 ± 0.2%ID/ml after 45 min and further to 0.8 ± 0.1%ID/ml after 90 min.

In order to confirm reversible, DAT specific binding, a displacement study was conducted with the structurally unrelated DAT ligand GBR12909 (1.5 mg/kg) and [^{18}F]PR04.MZ. In average, 80% of the bound radioactivity was displaced from the putamen, caudate nucleus and midbrain ROIs within 60 min post injection, thus confirming DAT-specific binding.

The test–retest reliability was calculated from the time activity curves.[16] Both scans showed good correlation (0.89). Hence, a reliability of 0.94 has been calculated using the split-halves method.

Blood and plasma analyses . Plasma–protein binding of [^{11}C]PR04.MZ was determined to assess the free fraction of the radiotracer in plasma (f_P).[22] Neostigmine (15 µl) was added to plasma samples to inhibit the acetylcholine esterase-mediated cleavage of the [^{11}C]methyl ester label.[18,19] It was found, that approximately 4.4% of the injected radiotracer was freely diffusible, that is, unbound, in the aqueous fraction of the plasma (Table 1). This is in the same range as reported for other DAT ligands including cocaine.[17] The high amount of [^{11}C]-**1** which is bound in plasma is possibly related to expression of the DAT on blood platelets.[17] Plasma metabolism of [^{11}C]-**1** was assessed via blood sampling throughout the PET scan.[17] The blood plasma was analysed and the percentage of intact tracer at each time-point was used to derive the plasma input functions of both radiotracers. [^{11}C]-**1** showed a rapid metabolism in the plasma, which is comparable to the findings in rats reported earlier. Only 39 ± 6% of the intact tracer were found in baboon plasma at 30 min p.i. (n = 3). A similar rapid metabolism has also been reported for PE2I, FECNT and LBT-999.[8,12] The value of PE2I and FECNT are somewhat confounded due to the presence of polar metabolites that enter the brain in rats.[7] No radioactive metabolites of [^{11}C]-**1** were found in homogenised Sprague–Dawley rat brain at 60 min p.i. Instead, more than 95% of the intact tracer was present in the brain at this time-point, as determined by HPLC. For comparison, no metabolite of [^{18}F]-**1** was found in homogenised Wistar rat brain up to 120 min p.i.[18,19] N-dealkylation, a metabolic pathway for tropanes as shown in N-[^{11}C]cocaine and [^{18}F]FECNT,[7,14,19] might lead to a labelled metabolite of [^{11}C]-**1** capable of entering the brain. However, the presence of N-desalkyl-[^{11}C]-**1** in the plasma was ruled out by liquid chromatography in blood samples. This hints on an increased stability towards N-desalkylation compared to N-[^{11}C]cocaine and [^{18}F]FECNT. The metabolite-corrected blood input data as well as reference tissue data from the cerebellum ROI was used for kinetic modelling and calculation of distribution volumes (V_T) and binding potentials (BP_{ND})[20–22] (Table 2).

Distribution of [^{11}C]-**1** in the baboon brain parallels the cerebral distributions reported for FECNT, PE2I and LBT-999[7,8,12,23] in rhesus monkey (macaca mulatta) Marked uptake of these PET

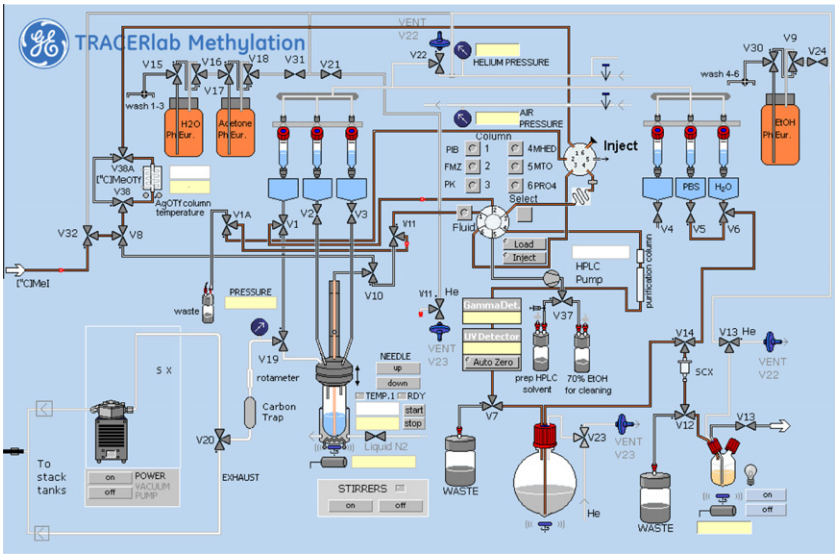

Scheme 2. Process scheme for [^{11}C]PR04.MZ production on a GE Tracerlab FX$_C$ synthesis module, adapted to the captive solvent method (loop method). Follow the orange lines for the mass stream leading from [^{11}C]MeI to [^{11}C]PR04.MZ.

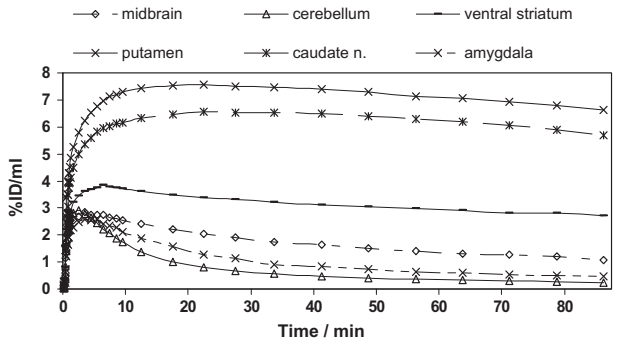

Figure 1. Mean time activity curves for [^{11}C]PR04.MZ and [^{18}F]PR04.MZ in various baboon brain regions.

tracers and [^{11}C]-**1** into the striatum is in good accordance with the pronounced expression of the DAT in this brain region. Moreover, uptake into the midbrain comprising of the substantia nigra and the ventral tegmental area, two brain regions with profound DAT expression is clearly detectable in the primate brain with PE2I or LBT-999[23] and also with [^{11}C]-**1**. In terms of quantification, essentially equivalent V_T-ratios and BP$_{ND}$ values are obtained for [^{18}F]FECNT, [^{11}C]PE2I, [^{18}F]LBT-999 and [^{11}C]-**1** in non-human primates.[23] However, whereas the formation of blood brain barrier penetrating metabolites complicates PET studies with [^{18}F]FECNT and [^{11}C]PE2I, there is no indication of adverse metabolism in [^{11}C]-**1** so far. Apart from that, [^{11}C]-**1** exhibits very low non-specific binding and insignificant retention in brain regions with low DAT-density, such as the cerebellum was observed in the present study (Fig. 2).

Compound [^{11}C]-**1** is significantly retained within the midbrain (midbrain-to-cerebellum ratios: 4.6 ± 0.3, 90 min p.i). The binding equilibrium necessary for quantitative studies within this brain region is reached 20 min p.i. [^{11}C]-**1** displays good test–retest reliability and visualises the DAT-containing brain regions in and outside of the striatum in the primate brain. Thus, [^{18}F]-**1** permits assessment of distribution and routine application of the tracer in molecular diagnostics, whereas [^{11}C]-**1** is well suited for multiple injection studies in the same subject on the same day. The visualisation of the extra-striatal DAT in the midbrain might account for a better understanding of dopaminergic contributions to psychiatric and neurodegenerative disorders with PET. In this regard, the absence of blood brain barrier penetrating metabolites, low non-specific binding and fast washout from the cerebellum warrant the use of this region as reference tissue for kinetic modelling.

Table 2
Distribution volumes (V_T), binding potentials (BP$_{ND}$), influx constant K_1 and efflux constant k_2 from two compartment kinetic modelling

[^{11}C]PR04.MZ	V_T in mlcm^{-3}	BP$_{ND}$ in mlcm^{-3}	K_1 in mlcm^{-3}min^{-1}	k_2 in min^{-1}
Cerebellum	3.9	0	0.144	0.036
Midbrain	14.4	2.7	0.064	0.016
Ventral striatum	35.8	8.2	0.030	0.0076
Caudate n.	118.0	29.3	0.017	0.004
Putamen	147.6	36.8	0.015	0.004

Values from three independent studies with [^{11}C]PR04.MZ.

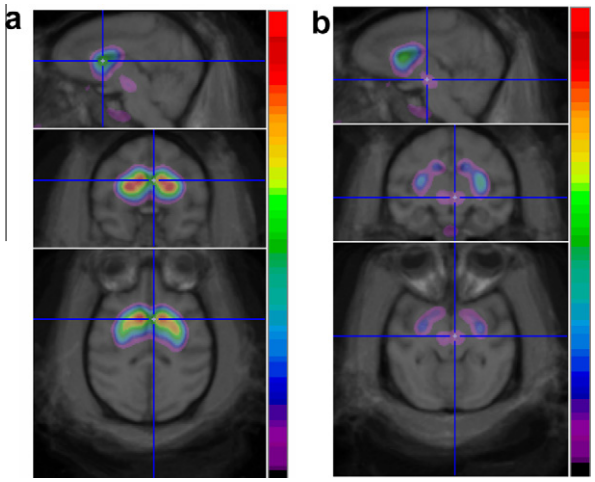

Figure 2. Sagittal, coronal and transversal view of PET/MR-fusion images of the basal ganglia (left, a) and the midbrain region (right, b). Results are mean values from two test–retest scans in the same baboon ±1 SD.

A reliable automated radiosynthesis of [^{11}C]PR04.MZ using GMP compliant equipment and reagents has been established. The tracer can be produced in high quality and high specific activity, appropriate for human studies. The characterisation of the tracer in baboons again confirmed that [^{11}C]PR04.MZ is a selective radioligand, suitable for the exploration of DAT binding sites. [^{11}C]-**1** shows a rapid, relatively high uptake into the DAT-containing brain regions and low non-specific binding. The radiotracer is particularly well suited for the exploration of the extra-striatal DAT, that is, the low DAT concentration in the midbrain. In this brain region binding equilibrium is already reached 20 min into the PET scan. The radiotracer is rapidly metabolised, though no labelled metabolite was detected in homogenised rat brains, 60 min into the PET scan. The ROI data shows good correlation in between the test–retest scans and the calculated test–retest reliability was 0.94. [^{11}C]-**1** has shown promising results as selective markers of the presynaptic dopamine transporter. With the reliable visualisation of extra-striatal dopaminergic neurons and no indication on labelled metabolites, the tracer provides excellent potential for translation into man.

Acknowledgements

This work was supported by the DFG [Ro 985/21], the US DoE and the Fonds der Chemischen Industrie.

References and notes

1. Hersch, S. M.; Yi, H.; Heilman, C. J.; Edwards, R. H.; Levey, A. I. *J. Comp. Neurol.* **1997**, *388*, 211.
2. Laakso, A.; Hietala, J. *Curr. Pharm. Des.* **2000**, *6*, 1611.
3. Marshall, V.; Grosset, D. *Mov. Disord.* **2003**, *18*, 1415.
4. Bergstrom, K. A.; Tupala, E.; Tiihonen, J. *Pharmacol. Toxicol.* **2001**, *88*, 287.
5. Laruelle, M.; Slifstein, M.; Huang, Y. *Methods* **2002**, *27*, 287.
6. Okada, T.; Shimada, S.; Sato, K.; Schloss, P.; Watanabe, Y.; Itoh, Y. *Nucl. Med. Biol.* **1998**, *25*, 53.
7. (a) Shetty, H. U.; Zoghbi, S. S.; Liow, J. S.; Ichise, M.; Hong, J. S.; Musachio, J. L.; Seneca, N.; Halldin, C.; Seidel, J.; Innis, R. B.; Pike, V. W. *Eur. J. Nucl. Med. Mol. Imaging* **2007**, *34*, 667; (b) Zoghbi, S. S.; Shetty, H. U.; Ichise, M.; Fujita, M.; Imaizumi, M.; Liow, J.-S.; Shah, J.; Musachio, J. L.; Pike, V. W.; Innis, R. B. *J. Nucl. Med.* **2006**, *47*, 520; (c) Kilbourn, M. R.; Carey, J. E.; Koeppe, R. A.; Haka, M. S.; Hutchins, G. D.; Sherman, P. S.; Kuhl, D. E. *Int. J. Rad. Appl. Instrum. B.* **1989**, *16*, 569; (d) Yaqub, M.; Boellaard, R.; van Berckel, B. N. M.; Ponsen, M. M.; Lubberink, M.; Windhorst, A. D.; Berendse, H. W.; Lammertsma, A. A. *J. Cerebr. Blood Flow Metab.* **2006**, *27*, 1397.
8. Goodman, M. M.; Kilts, C. D.; Keil, R.; Shi, B.; Martarello, L.; Xing, D.; Votaw, J.; Ely, T. D.; Lambert, P.; Owens, M. J.; Camp, V. M.; Malveaux, E.; Hoffman, J. M. *Nucl. Med. Biol.* **2000**, *27*, 1.
9. (a) Jucaite, A.; Odano, I.; Olsson, H.; Pauli, S.; Halldin, C.; Farde, L. *Eur. J. Nucl. Med. Mol. Imaging* **2006**, *33*, 657; (b) Ernst, M.; Zametkin, A. J.; Matochik, J. A.; Pascualvaca, D.; Jons, P. A.; Cohen, R. M. *Am. J. Psychiatry* **1999**, *156*, 1209.
10. (a) Riss, P. J.; Hummerich, R.; Schloss, P. *Org. Biomol. Chem.* **2009**, *7*, 2688; (b) Riss, P. J.; Debus, F.; Hummerich, R.; Schloss, P.; Lueddens, H.; Roesch, F. *ChemMedChem* **2009**, *4*, 1480; (c) Riss, P. J.; Hooker, M. J.; Alexoff, D.; Kim, S.-W.; Fowler, J. S.; Roesch, F. *Bioorg. Med. Chem. Lett.* **2009**, *19*, 4343; (d) Riss, P. J.; Roesch, F. *Bioorg. Med. Chem.* **2009**, *17*, 7630.
11. Wilson, A. A.; Garcia, A.; Jin, L.; Houle, S. *Nucl. Med. Biol.* **2000**, *27*, 529.
12. (a) Chalon, S.; Garreau, L.; Emond, P.; Zimmer, L.; Vilar, M.-P.; Besnard, J.-C.; Guilloteau, D. *J. Pharmacol. Exp. Ther.* **1999**, *291*, 648; (b) Chalon, S.; Hall, H.; Saba, W.; Garreau, L.; Dollé, F.; Halldin, C.; Emond, P.; Bottlaender, M.; Deloye, J. B.; Helfenbein, J.; Madelmont, J. C.; Bodard, S.; Mincheva, Z.; Besnard, J. C.; Guilloteau, D. *J. Pharmacol. Exp. Ther.* **2006**, *317*, 147; (c) Saba, W.; Valette, H.; Schöllhorn-Peyronneau, M.-A.; Coulon, C.; Ottaviani, M.; Chalon, S.; Dolle, F.; Emond, P.; Halldin, C.; Helfenbein, J.; Madelmont, J. C.; Deloye, J. B.; Guilloteau, D.; Bottlaender, M. *Synapse* **2007**, *61*, 17.
13. OECD guidelines for the testing of chemicals. (2004). Partition Coefficient (*n*-octanol/water) High Performance Liquid chromatography (HPLC) Method. #117.
14. Ambre, J.; Fischman, M.; Ruo, T.-I. *J. Anal. Toxicol.* **1984**, *8*, 23–25.
15. Schwartz, H. J.; Johnson, D. *Clin. Toxicol.* **1996**, *34*, 77.
16. Carmines, E. G.; Zeller, R. A. *Reliability and Validity Assessment*; Sage Publications: Thousand Oaks, CA, 1979.
17. (a) Frankhauser, P.; Grimmer, Y.; Bugert, P.; Deuschle, M.; Schmidt, M.; Schloss, P. *Neurosci. Lett.* **2006**, *399*, 1997; (b) Marazziti, D.; Baroni, S.; Fabbrini, L.; Italiani, P.; Catena, M.; Dell'Osso, B.; Betti, L.; Giannaccini, G.; Lucacchini, A.; Cassano, G. *Neurochem. Res.* **2006**, *31*, 361.
18. (a) Alexoff, D. L.; Shea, C.; Fowler, J. S.; King, P.; Gatley, S. J.; Wolf, A. P. *Nucl. Med. Biol.* **1995**, *22*, 893; (b) Gatley, S. J.; Yu, D.-W.; Fowler, J. S.; McGregor, R. R.; Schlyer, D. J.; Dewey, S.; Wolf, A. P.; Martin, T.; Shea, C.; Volkow, N. *J. Neurochem.* **1994**, *62*, 1154.
19. Fowler, J. S.; Volkow, N. D.; Wolf, A. P.; Dewey, S.; Schlyer, D. J.; McGregor, R. R.; Hitzeman, R.; Logan, J.; Bendriem, B.; Gatley, S. J.; Christman, D. *Synapse* **1998**, *4*, 371.
20. Logan, J. *Nucl. Med. Biol.* **2000**, *27*, 661.
21. Logan, J.; Fowler, J. S.; Volkow, N. D.; Wang, G.-J.; Ding, Y.-S.; Alexoff, D. L. *J. Cerebr. Blood Flow Metab.* **1996**, *16*, 834.
22. Innis, R. B.; Cunningham, V. J.; Delforge, J.; Fujita, M.; Gjedde, A.; Gunn, R. N.; Holden, J.; Houle, J.; Huang, S.-C.; Ichise, M.; Iida, H.; Ito, H.; Kimura, Y.; Koeppe, R. A.; Knudsen, G. M.; Knuuti, J.; Lammertsma, A. A.; Laruelle, M.; Logan, J.; Maguire, R. P.; Mintun, M. A.; Morris, E. D.; Parsey, R.; Price, J. C.; Slifstein, M.; Sossi, V.; Suhara, T.; Votaw, J. R.; Wong, D. F.; Carson, R. E. *J. Cerebr Blood Flow Metab.* **2007**, *27*, 1533.
23. (a) Varrone, A.; Tóth, M.; Steiger, C.; Takano, A.; Guilloteau, D.; Ichise, M.; Gulyás, B.; Halldin, C. *J. Nucl. Med.* **2011**, *52*, 132–139; (b) Varrone, A.; Stepanov, V.; Nakao, R.; Tóth, M.; Gulyás, B.; Emond, P.; Deloye, J. B.; Vercouillie, J.; Stabin, M. G.; Jonsson, C.; Guilloteau, D.; Halldin, C. *J. Nucl. Med.* **2011**, *52*, 13–1321.
24. QC-results from five independent productions of [^{11}C]PR04.MZ; HPLC conditions: MeCN-50 mM ammonium acetate solution, 6:4, pH 4.5, 1 ml min^{-1}, Phenomenex Luna RP18(2), 5 μ, 250 × 4.6 mm, t_r = 13.8 ± 0.4 min, UV detection at 254 nm; the radiochemical yield was calculated from the estimated irradiation yield.